Epitaxial growth and dielectric properties of $Pb_{0.4}Sr_{0.6}TiO_3$ thin films on (00*l*)-oriented metallic $Li_{0.3}Ni_{0.7}O_2$ coated MgO substrates

X. T. Li and P. Y. Du[a)]
State Key Laboratory of Silicon Mzaterials, Zhejiang Univrsity, Hangzhou 310027, People's Republic of China and Department of Materials Science and Engineering, Zhejiang University, Hangzhou 310027, People's Republic of China

C. L. Mak and K. H. Wong
Department of Applied Physics and Materials Research Center, The Hong Kong Polytechnic University, Hung Hom, Hong Kong, People's Republic of China

(Received 23 March 2007; accepted 5 June 2007; published online 26 June 2007)

Highly (00*l*)-oriented $Li_{0.3}Ni_{0.7}O_2$ thin films have been fabricated on (001) MgO substrates by pulsed laser deposition. The $Pb_{0.4}Sr_{0.6}TiO_3$ (PST40) thin film deposited subsequently also shows a significant (00*l*)-oriented texture. Both the PST40 and $Li_{0.3}Ni_{0.7}O_2$ have good epitaxial behavior. The epitaxial growth of the PST40 thin film is more perfect with the $Li_{0.3}Ni_{0.7}O_2$ buffer layer due to the less distortion in the film. The dielectric tunability of the PST40 thin film with $Li_{0.3}Ni_{0.7}O_2$ buffer layer therefore reaches 70%, which is 75% higher than that without $Li_{0.3}Ni_{0.7}O_2$ buffer layer, and the dielectric loss of the PST40 thin film is 0.06. © *2007 American Institute of Physics*.
[DOI: 10.1063/1.2752532]

Dielectric thin films are attractive materials for the applications in tunable microwave devices such as electrically tunable mixers, phase shifter, resonator, filter, etc.[1–5] Also, $Pb_xSr_{1-x}TiO_3$ (PST) is a ferroelectric solid solution between $PbTiO_3$ and $SrTiO_3$ with cubic or tetragonal structure, and its physical properties vary depending on its composition.[6–8] Recently the demand for thin films processing has increased because of miniaturization of electric components for integrated devices.[9] The PST thin films, especially highly *c*-axis oriented PST thin film, are expected to be better for tunable microwave applications such as dielectric properties and nonlinear polarization applications.

Conducting metallic oxides, such as $LaNiO_3$, $SrRuO_3$, and $La_{0.5}Sr_{0.5}CoO_3$, are considered to be a promising alternate for electrodes because they have a better crystallographic compatibility with the perovskite phase layer at the interface compared to Pt electrodes.[10–12] $LaNiO_3$ have been widely used as a conducting material for *c*-axis PST thin film on Si (001) substrates due to its proper lattice constant.[13] However, because $LaNiO_3$ has a high orientation of (*ll*0) on MgO substrate,[14] it cannot be used for *c*-axis PST thin film on MgO (001). In fact, MgO (001) substrate is one of the most important transparent substrates for microwave application due to its temperature-independent dielectric constant ($\varepsilon=10$) and low dielectric loss tangent ($\tan\delta<10^{-5}$ at 77 K and 10 GHz).[15] Therefore, an appropriate buffer layer is required for the *c*-axis PST on MgO (001) substrate.

Being compared with $LaNiO_3$ ($c=0.382$ nm), $Li_xNi_{1-x}O_2$, which is a metallic oxide of cubic structure with a lattice parameter of 0.414 nm,[16] matches well with both the ferroelectric thin films such as PST ($c=0.395$ nm) and the commonly used metallic oxide substrates such as MgO ($c=0.420$ nm). In this work, $Li_{0.3}Ni_{0.7}O_2$ is employed as an electrode as well as a buffer layer for the growth of highly oriented ferroelectric thin film used in tunable devices. The structural properties and dielectric properties are investigated for the highly (00*l*)-oriented PST40 thin films grown on $Li_{0.3}Ni_{0.7}O_2$ coated MgO substrates fabricated by pulsed laser deposition (PLD) technique. On the basis of our results, we demonstrate that $Li_{0.3}Ni_{0.7}O_2$ is an ideal candidate to be used as both a transparent bottom electrode both a buffer layer for growing highly oriented ferroelectric thin films.

$Li_{0.3}Ni_{0.7}O_2$ targets were prepared by sintering Li_2CO_3 and NiO powders at 900 °C for 2.5 h. To avoid lithium deficiency, nominal Li/Ni ratio of 30/70 plus 20 at. % excess Li was used. Deposition was carried out using a KrF excimer laser operated at a power density of 5 J/cm^2 and a laser repetition rate of 10 Hz. The $Li_{0.3}Ni_{0.7}O_2$ film was deposited at a substrate temperature of 600 °C under an oxygen partial pressure of 100 mTorr. On top of the $Li_{0.3}Ni_{0.7}O_2$ coated MgO substrates, we *in situ* deposited PST40 thin films. The targets of PST thin film were prepared by sintering PbO, $SrCO_3$, and TiO_2 powders at 900 °C for 2.5 h. The nominal Pb/Sr composition ratio of the target is 40/60 with 20 at. % excess of Pb to compensate for the volatilization of Pb. The optimal growth conditions of PST40 on $Li_{0.3}Ni_{0.7}O_2$/MgO substrate were found to be deposition temperature of 780 °C and oxygen pressure of 200 mTorr. After deposition, the PST40/$Li_{0.3}Ni_{0.7}O_2$ films were kept at the deposited temperature for 30 min before naturally cooling down to room temperature. In order to make sure for the superiority of the $Li_{0.3}Ni_{0.7}O_2$ buffer layer, PST40 thin films without $Li_{0.3}Ni_{0.7}O_2$ were also deposited on the (001) MgO substrates at the same time.

The crystalline structures of the films were analyzed by x-ray diffraction (XRD) with Cu $K\alpha$ radiation. The epitaxial quality of the $Li_{0.3}Ni_{0.7}O_2$ and PST40 films was characterized by x-ray rocking curve and Φ scans. Scanning electron microscopy (SEM) was used to examine the surface morphologies and cross-sectional profiles of these films. The *I*-*V* characteristic and the transmittance of the bottom electrode $Li_{0.3}Ni_{0.7}O_2$ were measured using a KE6517A impedance analyzer and an ultraviolet spectrometer, respectively. The

a)Electronic mail: dupy@zju.edu.cn

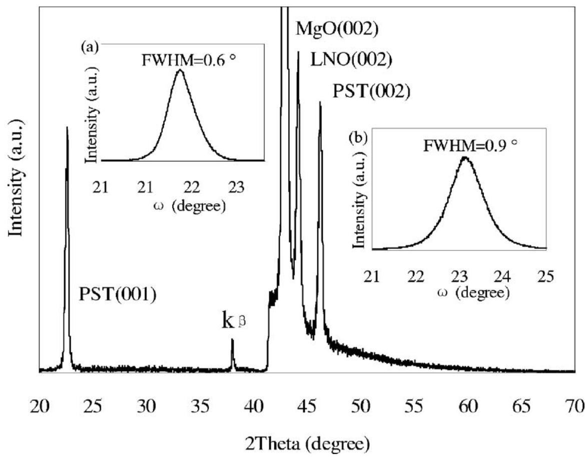

FIG. 1. XRD patterns of PST40 thin films deposited on $Li_{0.3}Ni_{0.7}O_2$ coated MgO substrates and annealed at 780 °C. The inset is the full width half maximum of the rocking curves of (a) $Li_{0.3}Ni_{0.7}O_2$ films and (b) PST40 thin films.

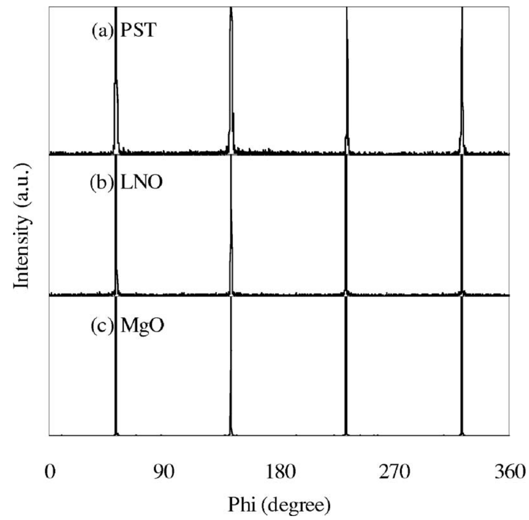

FIG. 2. Φ-scan patterns for a highly textured PST40 thin film deposited on $Li_{0.3}Ni_{0.7}O_2$ coated MgO (001) substrates.

dielectric properties of the PST40 films were measured by using a precision impedance analyzer.

Figure 1 shows the θ-2θ XRD patterns of the $Pb_{0.4}Sr_{0.6}TiO_3$ thin film grown on the $Li_{0.3}Ni_{0.7}O_2$ coated MgO substrate by PLD technique at 780 °C. The bottom electrode $Li_{0.3}Ni_{0.7}O_2$ was prepared at 600 °C on (001) MgO substrates. Vertical step near the strong reflections of MgO (002) has originated from Ni filter. For $Li_{0.3}Ni_{0.7}O_2$ layer, only peaks from (00*l*) $Li_{0.3}Ni_{0.7}O_2$ and (00*l*) MgO reflections appear, indicating that the as-grown thin film is *c*-axis oriented. For PST40 thin film, the reflections of PST (001) and PST (002) are identified and no trace of other reflections is observed, which show no significant difference to the PST40 deposited on the (001) MgO substrate. The inset of Figs. 1(a) and 1(b) illustrate rocking curves of the (002) peak for the (00*l*)-oriented $Li_{0.3}Ni_{0.7}O_2$ layer and PST40 thin films, respectively. The full width at half maximum of $Li_{0.3}Ni_{0.7}O_2$ and PST40 are about 0.6°and 0.9°, respectively, showing that the tilt distributions of the thin film's crystallites are very narrow.

In-plane orientations of the $Li_{0.3}Ni_{0.7}O_2$ and PST40 films are determined by Φ scans of the {111} families. The azimuthal (111) diffraction patterns of $Li_{0.3}Ni_{0.7}O_2$ and MgO in the vicinity of the main feature are shown in Figs. 2(b) and 2(c), respectively. The four peaks having a 90° interval to each other indicated the fourfold symmetry of MgO and $Li_{0.3}Ni_{0.7}O_2$. This means that the $Li_{0.3}Ni_{0.7}O_2$ thin films are cube-on-cube grown on MgO substrates. Figure 2(a) shows that the clear four features at 90° interval to each other were also found for PST40 films. Thus, the epitaxial relationship of (001) PST‖(001)$Li_{0.3}Ni_{0.7}O_2$‖(001) MgO is obtained.

The surface morphologies of $Li_{0.3}Ni_{0.7}O_2$ and PST40 are shown in Figs. 3(a) and 3(b), respectively. Both $Li_{0.3}Ni_{0.7}O_2$ and PST40 thin film surfaces are dense, smooth, and crack-free, indicating the good quality of the thin films. The cross section of the PST40 thin film deposited on $Li_{0.3}Ni_{0.7}O_2$ coated MgO substrates is shown in Fig. 3(c). The thicknesses of the PST40 and $Li_{0.3}Ni_{0.7}O_2$ layers are about 900 and 150 nm, respectively.

The conductivity of the bottom $Li_{0.3}Ni_{0.7}O_2$ electrode was examined by measuring the *I*-*V* curve, which is shown in Fig. 4(a). The current is linearly increased with applied voltage in the region of $V=-20-20$ V. The conductivity is estimated to be 2.5×10^{-3} Ω m. This conductivity makes the highly (00*l*)-oriented $Li_{0.3}Ni_{0.7}O_2$ an ideal bottom electrode. In addition, its transmission spectra have been measured in the wavelength ranging from 0.2 to 0.8 μm using a two-beam spectrophotometer (Shimadazu, UV.2101). The measured transmittance profile is shown in Fig. 4(b). The optical transmittance of the thin film decreased to zero near 300 nm due to the interband transitions. The maximum transmittance is about 35% at 0.8 μm. Hence, the $Li_{0.3}Ni_{0.7}O_2$ thin film is also a good candidate as the transparent bottom electrode.

The typical dc field dependence of the capacitance (C_p) as well as the dielectric loss (tan δ) for the highly epitaxial PST40 thin films were measured at 100 kHz, as shown in Fig. 5(a). The capacitances of the thin films decreased with an increase in dc bias at 100 kHz, which was well fitted to

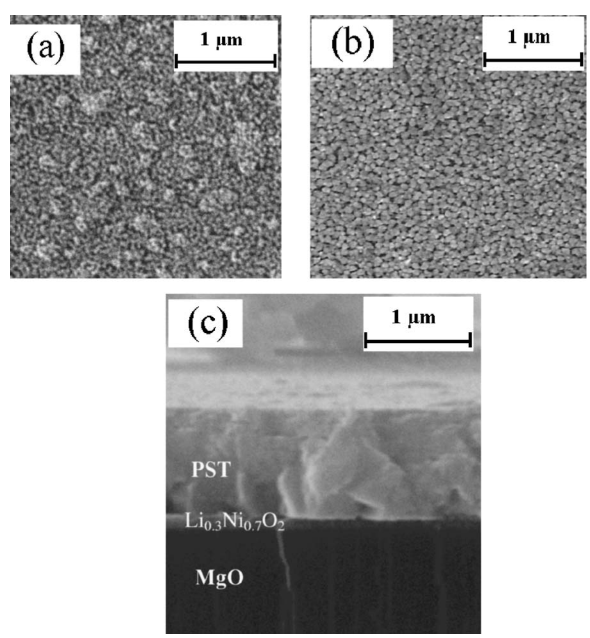

FIG. 3. Surface SEM images of (a) bottom electrode $Li_{0.3}Ni_{0.7}O_2$, (b) PST40 thin film deposited on $Li_{0.3}Ni_{0.7}O_2$/MgO, and (c) cross-sectional SEM images of PST40 thin film deposited on $Li_{0.3}Ni_{0.7}O_2$ coated MgO (001) substrates.

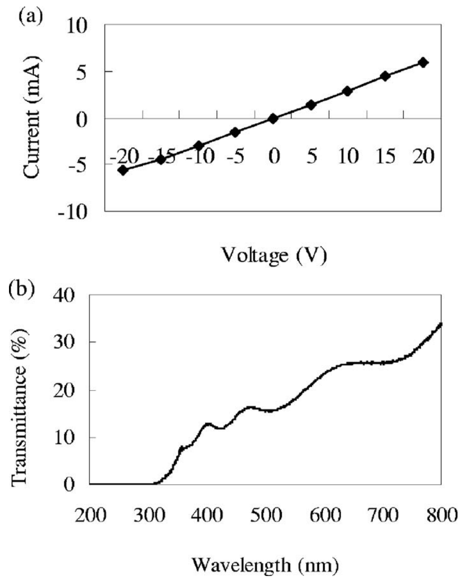

FIG. 4. (a) *I-V* characteristic and (b) transmission spectra of the bottom electrode $Li_{0.3}Ni_{0.7}O_2$ deposited on MgO substrates at 600 °C.

the Lorentz function.[17] The dielectric loss was about 0.06, which is small enough for the tunable applications. As it is known, the tunability is defined as tunability $=(C_{\text{zero bias}}-C_{\text{dc bias}})/C_{\text{zero bias}}\times 100\%$. Figure 5(b) shows the tunabilities of the epitaxial PST40 thin films with and without the $Li_{0.3}Ni_{0.7}O_2$ buffer layer on MgO (001) substrates. The maximum tunabilities of about 70% (with $Li_{0.3}Ni_{0.7}O_2$) and 40% (without $Li_{0.3}Ni_{0.7}O_2$) appear, respectively, when the voltage range between 0 and $|20|$ V. The former is actually much higher than the latter. As we know, both PST40 thin films with and without the $Li_{0.3}Ni_{0.7}O_2$ buffer layer are epitaxial from the MgO (001). Although the PST thin film can epitaxially grow on the MgO (001) substrates.[18] The tunabiliy of the PST thin film is actually much lower than that of the PST thin film deposited on the $Li_{0.3}Ni_{0.7}O_2$ buffer layer. This is attributed to the lattice parameter of the PST thin film that is much closer to $Li_{0.3}Ni_{0.7}O_2$ ($c=0.414$ nm) than to MgO ($c=0.420$ nm). $Li_{0.3}Ni_{0.7}O_2$ also matches well with the MgO (001) substrate, and the epitaxial growth is perfect due to the small stress in the $Li_{0.3}Ni_{0.7}O_2$ on MgO. Therefore the PST thin film matches better with the perfect $Li_{0.3}Ni_{0.7}O_2$ thin film than MgO. That is to say, the stress between $Li_{0.3}Ni_{0.7}O_2$ and PST is smaller than that between MgO and PST. The $Li_{0.3}Ni_{0.7}O_2$ buffer layer can either increase the perfection of the thin film or restrain the deficiency in the PST lattice induced by the MgO substrates. Hence, the tunabiliy of the PST thin film is improved significantly to as much as 70%. It is a little higher than the high quality barium strontium titanate thin film, whose tunability is usually exhibited within the range from about 50% to 60%.

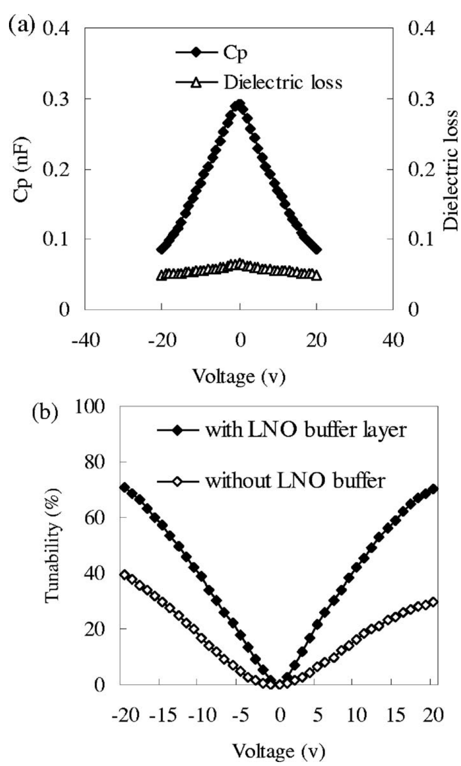

FIG. 5. (a) C_p and dielectric loss of PST40 thin film deposited on $Li_{0.3}Ni_{0.7}O_2$ coated MgO (001) substrates. (b) Tunabilities of PST40 thin film with and without $Li_{0.3}Ni_{0.7}O_2$ buffer layer.

In summary, (00*l*)-oriented $Li_{0.3}Ni_{0.7}O_2$ thin films have been grown on MgO substrates at 600 °C by PLD technique. These films are metalliclike and can be used as both the bottom electrode and buffer layer for the growth of textured ferroelectric thin films. This was demonstrated by successfully depositing PST40 films on $Li_{0.3}Ni_{0.7}O_2$ coated MgO substrates. Both $Li_{0.3}Ni_{0.7}O_2$ and PST40 film surfaces are dense, smooth, and crack-free. The tunability of the PST40 film is about 70% and the dielectric loss is about 0.06. These excellent results indicate that the highly epitaxial PST thin films are good candidates for tunable applications.

This work is supported by NSFC (Grant Nos. 50372057 and 50332030), and NKSTP (Grant No. 2002CB613302). It is also supported by a Research Grant (GU-098) of the Hong Kong Polytechnic University.

[1]L. A. Knauss, J. M. Pond, S. J. Horwitz, D. B. Chrisey, C. H. Mueller, and R. Treece, Appl. Phys. Lett. **69**, 25 (1992).
[2]H. D. Kang, J. H. Kim, J. H. Park, and K. H. Yoon, Mater. Res. Bull. **36**, 256 (2001).
[3]S. W. Liu, J. Chakhalian, Min Xiao, and C. L. Chen, Appl. Phys. Lett. **90**, 042901 (2007).
[4]M. W. Cole, W. D. Nothwang, C. Hubbard, E. Ngo, and M. Ervin, J. Appl. Phys. **93**, 9218 (2003).
[5]P. Y. Du, S. Sui, W. J. Weng, G. R. Han, and J. X. Wang, Acta Phys. Sin. **54**, 5411 (2005).
[6]K. T. Kim and C. I. Kim, Thin Solid Films **420-421**, 544 (2002).
[7]M. Jain, S. B. Majumder, R. Guo, A. S. Bhalla, and R. S. Katiyar, Mater. Lett. **56**, 692 (2002).
[8]Y. L. Liu, P. Y. Du, W. J. Weng, G. R. Han, and G. Shen, J. Inorg. Mater. **20**, 151 (2005).
[9]P. Y. Du, X. T. Li, Y. L. Liu, G. R. Han, and W. J. Weng, J. Eur. Ceram. Soc. **26**, 2147 (2006).
[10]H. N. Tsai, Y. C. Liang, and H. Y. Lee, J. Cryst. Growth **284**, 65 (2005).
[11]R. J. Kennedy, R. Madden, and P. A. Stampe, J. Phys. D **34**, 1853 (2001).
[12]G. P. Luo, Y. S. Wang, S. Y. Chen, A. K. Heilman, C. L. Chen, C. W. Chu, Y. Liou, and N. B. Ming, Appl. Phys. Lett. **76**, 1908 (2000).
[13]K. T. Kim and C. I. Kim, Thin Solid Films **447–448**, 651 (2004).
[14]L. Zheng, J. Zhu, Y. Zhang, S. W. Jiang, Y. R. Li, X. Huawei, and J. L. Li, Appl. Surf. Sci. **252**, 3609 (2006).
[15]V. Boffa, T. Petrisor, L. Ciontea, U. Gambardella, and S. Barbanera, Physica C **260**, 111 (1996).
[16]P. Kalyani and N. Kalaiselvi, Sci. Technol. Adv. Mater. **6**, 689 (2005).
[17]H. Li, A. L. Royburd, and S. P. Alpay, Appl. Phys. Lett. **78**, 2354 (2001).
[18]S. W. Liu, J. Weaver, Z. Yuan, W. Donner, C. L. Chen, J. C. Jiang, E. I. Meletis, W. Chang, S. W. Kirchoefer, J. Horwitz, and A. Bhalla, Appl. Phys. Lett. **87**, 142905 (2005).